Non-Gaussian statistics of extreme events in stimulated Raman scattering: The role of coherent memory and source noise

Yashar E. Monfared and Sergey A. Ponomarenko*
Department of Electrical and Computer Engineering, Dalhousie University, Halifax, Nova Scotia, Canada B3J 2X4
(Received 14 July 2017; published 9 October 2017)

We explore theoretically and numerically extreme event excitation in stimulated Raman scattering in gases. We consider gas-filled hollow-core photonic crystal fibers as a particular system realization. We show that moderate amplitude pump fluctuations obeying Gaussian statistics lead to the emergence of heavy-tailed non-Gaussian statistics as coherent seed Stokes pulses are amplified on propagation along the fiber. We reveal the crucial role that coherent memory effects play in causing non-Gaussian statistics of the system. We discover that extreme events can occur even at the initial stage of stimulated Raman scattering when one can neglect energy depletion of an intense, strongly fluctuating Gaussian pump source. Our analytical results in the undepleted pump approximation explicitly illustrate power-law probability density generation as the input pump noise is transferred to the output Stokes pulses.

DOI: 10.1103/PhysRevA.96.043817

I. INTRODUCTION

Rogue waves were originally observed as giant-amplitude waves occurring in high seas more frequently than predicted by Gaussian statistics [1–3]. The concept has subsequently been extended from oceanography to other areas of physics to describe waves of enormous amplitudes or, in general, extreme statistical events obeying heavy-tailed probability distributions [4]. Optics has proven to be an especially fertile ground for extreme event and, in particular, optical rogue wave (ORW) exploration [5,6]. To date, ORWs have been discovered theoretically and/or experimentally in supercontinuum generating optical fibers [7–9], optical cavities [10,11], passively mode-locked fiber lasers [12–14], erbium-doped fiber systems [15], Raman fiber amplifiers [16,17], spatiotemporal structures and laser filamentation [18–20], parametric processes [21], stimulated Raman scattering (SRS) [22], and even linear light propagation inside multimode fibers [23].

As ORWs are inherently statistical structures, their universal statistical signature is encapsulated in heavy-tailed non-Gaussian statistics of their amplitudes and/or powers. The non-Gaussian statistics emergence in nonlinear media has been a central theme of the burgeoning field of nonlinear statistical optics [24]. Specifically, non-Gaussian statistics generation and ORW excitation with a source field comprised of a coherent (cw) condensate component mixed with Gaussian noise has been extensively examined numerically [25–31] and experimentally [29,30] within the framework of the one-dimensional (1D) nonlinear Schrödinger equation (NLSE) [32]. The particulars of system statistics were shown to be very sensitive to initial conditions, strongly depending on the ratio of the condensate to random component amplitudes and the coherence time of the source [25,26,31]. Recently, the generation of highly non-Gaussian, heavy-tailed probability distributions has been numerically discovered and explored in SRS [22].

The two models just mentioned differ profoundly in many respects. While the first encompasses a class of weakly nonlinear wave systems with instantaneous response (no memory), governed by the integrable 1D NLSE, the second features a strong nonlinearity, long memory, and is, in general, nonintegrable. In this context, it is instructive to explore the role of coherent memory in causing non-Gaussian statistics of nonlinear systems. Stimulated Raman scattering appears to be a suitable candidate to address this question because its coherent memory is controlled by relative magnitudes of a characteristic SRS interaction and the Raman medium relaxation times. In the limit of an infinitely long Raman relaxation time, the system has extremely long memory and the SRS equations are integrable [33,34]. Another fundamental issue concerns the source noise modeling in rogue-wave-generating systems.

In our previous work on statistical SRS [22], we examined the case of noisy Stokes input pulses, amplified by a coherent pump in a gas-filled hollow-core photonic crystal fiber (HCPCF). In this work we study the same system under the condition that seed Stokes pulses are perfectly coherent, but pump pulses carry fluctuations obeying thermal statistics. This type of noisy pump can be implemented with amplitude-modulated statistically stationary sources or with multimode lasers operating at a large number of uncorrelated modes, yielding thermal-like source statistics [35]. We show, in particular, that SRS with a noisy pump is conducive to non-Gaussian statistics generation. We demonstrate that the Stokes pulse power probability density function (PDF) acquires a long tail at the fiber exit. The PDF tail extent strongly increases as the system approaches the long-memory integrability limit. In sharp contrast to the previously studied SRS with noisy input Stokes pulses, the Stokes pulse statistics is virtually unaffected by the source coherence time. We examine separately the Stokes pulse area PDF behavior in the undepleted pump approximation regime. We analytically demonstrate that the PDF exhibits powerlike behavior, failing to attain finite moments over fairly short propagation distances. This behavior points to the feasibility of ORW excitation over remarkably short distances in this SRS regime. We stress that this conclusion is independent of the initial Stokes pulse profile because our analytical theory gives a universal PDF in the undepleted pump approximation.

*serpo@dal.ca

This work is organized as follows. In the next section we introduce our theoretical model, including key dimensionless parameters describing the SRS physics. We formulate the statistical ensemble of fluctuating pump pulses in Sec. III. We then present our analytical theory in the undepleted pump approximation in Sec. IV. Next we present the results of our numerical simulations in Sec. V. Finally, we summarize our findings in Sec. VI.

II. THEORETICAL MODEL AND KEY DIMENSIONLESS PARAMETERS

We consider stimulated Raman scattering in a gas sample of molecular hydrogen, filling the core of a HCPCF. The fiber is assumed to be designed such that only the pump and the first Stokes modes lie within the fiber transparency window. In the usual weak excitation limit, the governing SRS equations in the copropagating geometry can be written in the dimensionless variables as [22]

$$\partial_Z \mathcal{E}_p = i\kappa\sigma\mathcal{E}_s, \tag{1}$$

$$\partial_Z \mathcal{E}_s = i\kappa^{-1}\sigma^*\mathcal{E}_p, \tag{2}$$

and

$$\partial_T \sigma = -\Gamma\sigma + i\mathcal{E}_p\mathcal{E}_s^*. \tag{3}$$

Here we introduced dimensionless pump and Stokes pulse amplitudes $\mathcal{E}_p$ and $\mathcal{E}_s$; the distance and time are scaled to the characteristic SRS interaction length and time, respectively, $Z = z/L_{\mathrm{SRS}}$ and $T = \tau/T_{\mathrm{SRS}}$, where $\tau = t - z/v_g$ is a time coordinate in the reference frame moving with the pulse group velocity v_g.

The characteristic SRS interaction length and time scales are defined as

$$L_{\mathrm{SRS}} = \left(\frac{2\epsilon_0 c}{N r_{\mathrm{eff}}}\right)\sqrt{\frac{n_p n_s}{\omega_p \omega_s}} \tag{4}$$

and

$$T_{\mathrm{SRS}} = \left(\frac{2\hbar\epsilon_0 c n_p}{r_{\mathrm{eff}}\langle I_{p0}\rangle}\right). \tag{5}$$

Here $\omega_{p,s}$ and $n_{p,s}$ are the carrier frequencies and refractive indices of the pump and Stokes pulses, respectively, N is a medium density, $\langle I_{p0}\rangle$ is a peak average pump intensity at the source, the angular brackets denoting ensemble averaging, and $r_{\mathrm{eff}} = \frac{1}{\hbar}\sum_i \frac{d_{3i}d_{i1}}{\omega_{i3}+\omega_{i1}-\omega_p-\omega_s}$ is a Raman transition dipole matrix element at the exact Raman resonance [36,37].

Further, we introduced $\kappa = \sqrt{\omega_p n_s/\omega_s n_p}$ and a coherent memory parameter Γ. The latter, defined as

$$\Gamma = \gamma\, T_{\mathrm{SRS}}, \tag{6}$$

where γ is a medium dipole phase relaxation rate, determines the extent of system memory and the system proximity to the integrability limit. Indeed, whenever $\Gamma \ll 1$, the SRS is highly transient with an extremely long memory time and its governing equations approach the mathematical integrability limit $\Gamma = 0$, first discussed in Refs. [33,34]. Thus, Γ is a key dimensionless parameter of the system as its magnitude distinguishes quasi-cw, $\Gamma \gg 1$, from transient, $\Gamma \ll 1$, SRS regimes. While SRS in the former regime has a relatively short memory, it is described by nearly integrable equations with long memory in the transient regime.

We stress that the magnitude of Γ demarcates the boundary between quasi-cw and transient SRS regimes in the nonlinear domain where pump depletion is no longer negligible. One should then exercise caution employing the usual rule-of-thumb criterion classifying SRS with pump pulses much shorter than the Raman relaxation time as transient [38]. The latter criterion, based on quantum SRS theory in the undepleted pump approximation [39], can prove too restrictive in the nonlinear domain. Indeed, coherent oscillations of pump and Stokes pulse profiles, which are unambiguous signatures of the transient dynamics, have been vividly displayed in the recent SRS experiments with pulses as long as or even longer than the Raman relaxation time [40]. A typical period of such oscillations in Ref. [40] was of the order of $T_{\mathrm{SRS}} \ll \gamma^{-1}$, implying that $\Gamma \ll 1$.

III. INPUT PUMP AND STOKES PULSES AND STATISTICAL ENSEMBLE FORMULATION

We consider a pump source pulse composed of a coherent Gaussian and a random component such that

$$\mathcal{E}_p(T,0) = e^{-(T-T_0)^2/2T_*^2} + \Delta\mathcal{E}_p(T), \tag{7}$$

where T_0 is a (dimensionless) pulse peak time. Such a source pulse can be experimentally realized by coherently combining a Gaussian pulse with a partially coherent one at a beam splitter, for example. The partially coherent (random) component can be generated by time modulating a statistically stationary source employing an electro-optical modulator, operating on the basis of either a linear [41] or a quadratic [42] electro-optical effect. All this is readily achievable in the nanosecond pulse range, adequate for SRS in gas-filled HCPCFs. The input Stokes pulse field reads

$$\mathcal{E}_s(T,0) = \sqrt{\frac{n_p P_s}{n_s P_p}}\, e^{-(T-T_0)^2/2T_*^2}, \tag{8}$$

where $P_{p,s}$ are peak powers of the (coherent components of) pump and Stokes pulses and $n_{p,s}$ are the refractive indices at the pump ω_p and Stokes ω_s frequencies, respectively. Further, we assume the pump and Stokes pulses to have the same duration (in dimensionless units) T_* at the source. Such a Stokes source can be produced in a separate fiber using the pump coherent component and quantum noise as inputs. A coherent macroscopic Stokes pulse is then formed as quantum noise is "cleaned up" [43]. This Stokes input can then be transported back into the original fiber to study ORW formation in the amplification regime of SRS.

We express the mutual intensity of the random component $\Delta\mathcal{E}_p$ using a celebrated Gaussian Schell model (GSM) of statistical optics [44]. The GSM presumes that both the intensity and the temporal degree of coherence of the fluctuating part have Gaussian profiles. We assume, for simplicity, that the fluctuating and coherent components have the same width T_p at the source. The mutual intensity of the random component, defined as

$$\Gamma(T_1,T_2,0) \equiv \langle \Delta\mathcal{E}_p^*(T_1,0)\Delta\mathcal{E}_p(T_2,0)\rangle, \tag{9}$$

can then be written as

$$\Gamma(T_1,T_2,0) = \left(\frac{\Delta P_p}{P_p}\right)\exp\left[-\frac{(T_1-T_0)^2+(T_2-T_0)^2}{2T_*^2}\right] \times \exp\left[-\frac{(T_1-T_2)^2}{2T_c^2}\right]. \quad (10)$$

Here $\Delta P_p/P_p$ is a ratio of the random to coherent component peak powers and T_c is a coherence time of the random component. It follows from Eq. (10) that the correlation spectrum of the GSM is also Gaussian. The GSM is a generic statistical source model, widely used in statistical optics [44]. For instance, a Gaussian correlation spectrum was shown to better approximate statistical properties of supercontinuum sources than does another commonly used model featuring a one-photon-per-mode spectrum [45].

We can now represent the random component of the source using the Karhunen-Loève expansion [46,47]

$$\Delta\mathcal{E}_p(T,0) = \sum_n c_n\psi_n(T), \quad (11)$$

where the random coefficients $\{c_n\}$ are statistically orthogonal such that

$$\langle c_n^* c_m\rangle = \lambda_n\delta_{mn}, \quad (12)$$

and the coherent modes are orthonormal, implying that

$$\int_{-\infty}^{\infty} dT\ \psi_n^*(T)\psi_m(T) = \delta_{mn}. \quad (13)$$

The mutual coherence function is then represented as a Mercer-type series in coherent modes as [44]

$$\Gamma(T_1,T_2,0) = \sum_n \lambda_n\psi_n^*(T_1)\psi_n(T_2). \quad (14)$$

The coherent modes $\{\psi_n\}$ are determined by solving the Fredholm integral equation

$$\int_{-\infty}^{\infty} dT_1\Gamma(T_1,T_2,0)\psi_n(T_1) = \lambda_n\psi_n(T_2). \quad (15)$$

In the GSM case, Eq. (15) can be analytically solved and all modes and the eigenvalues $\{\lambda_n\}$ determined such that [44]

$$\psi_n(T) = \left(\frac{2\xi}{\pi}\right)^{1/4}\left(\frac{1}{2^n n!}\right)^{1/2} H_n[\sqrt{2\xi}(T-T_0)]e^{-\xi(T-T_0)^2}, \quad (16)$$

where $H_n(x)$ is a Hermite polynomial of the order n and

$$\lambda_n = \sqrt{\pi}T_*\left(\frac{\Delta P_p}{P_p}\right)\frac{(\alpha+\xi)\beta^n}{(\alpha+\beta+\xi)^{n+1}}. \quad (17)$$

Here we introduced the notation

$$\alpha = \frac{1}{2T_*^2}, \quad \beta = \frac{1}{2T_c^2}, \quad (18)$$

and

$$\xi = \sqrt{\alpha^2+2\alpha\beta}. \quad (19)$$

We note that the mode powers (17) are normalized such that they add up to the total power of the random component (relative to the coherent component power).

To complete the ensemble description, we must specify the random amplitude statistics to any order such that it is consistent with Eq. (12). Expressing the complex random amplitudes $\{c_n\}$ in the polar form as

$$c_n = \sqrt{i_n}e^{i\phi_n}, \quad (20)$$

we stipulate that the complex amplitudes be independent random variables; the phases are assumed to be uniformly distributed in the interval $-\pi \leqslant \phi_n \leqslant \pi$, while the $\{i_n\}$ obey the exponential distribution such that

$$\mathcal{P}(i_n) = \frac{1}{\lambda_n}e^{-i_n/\lambda_n}, \quad i_n \geqslant 0. \quad (21)$$

If coherent modes correspond to natural oscillation modes of the source, such a source can be interpreted as a multimode laser source with each mode having a random phase and a strongly fluctuating power. The overall field at the source is a superposition of uncorrelated mode fields. As each mode obeys Gaussian statistics, the overall source PDF is guaranteed to be Gaussian (thermal-like) for any source coherence time T_c [22].

IV. UNDEPLETED PUMP APPROXIMATION

We first focus on the case of a very long, high-power pump pulse $t_p \gg t_s$ and $P_p \gg P_s$ such that the pump pulse can be treated as a plane wave. In the undepleted pump approximation (UPA), $\mathcal{E}_p = \text{const}$ and the SRS equations linearize. They can then be solved by a Fourier transform technique. Introducing a Fourier transform of the Stokes field

$$\tilde{\mathcal{E}}_s(\Omega,Z) = \int_{-\infty}^{\infty} dT\ e^{-i\Omega T}\mathcal{E}_s(T,Z), \quad (22)$$

where Ω is a frequency shift from the Stokes carrier and the Stokes pulse area,

$$\mathcal{A}_s(Z) = \int_{-\infty}^{\infty} dT\ \mathcal{E}_s(T,Z), \quad (23)$$

we can conclude at once that the latter is a component of the former at the carrier frequency, i.e.,

$$\mathcal{A}_s(Z) = \tilde{\mathcal{E}}_s(0,Z). \quad (24)$$

This observation allows us to quickly solve linearized equations (1)–(3) to obtain, for the area the expression,

$$\mathcal{A}_s(Z) = \mathcal{A}_{s0}\exp\left(\frac{|\mathcal{E}_p|^2 Z}{\kappa\Gamma}\right). \quad (25)$$

The area describes a universal dynamics of Stokes pulses: Whatever the initial pulse shape, the area grows exponentially.

Next we can determine the PDF of the area magnitude under the UPA. We assume a strong coherent pump with small intensity fluctuations such that the (dimensionless) intensity can be written as

$$|\mathcal{E}_p|^2 = 1 + i_p - \langle i_p\rangle \simeq 1 + i_p, \quad \langle i_p\rangle \ll 1. \quad (26)$$

This model is in sync with our general ensemble construct of Sec. III. The intensity fluctuations are specified by the PDF

$$\mathcal{P}(i_p) = \frac{1}{\langle i_p\rangle}e^{-i_p/\langle i_p\rangle}. \quad (27)$$

The area PDF is then given by the expression

$$\mathcal{P}(|\mathcal{A}_s|, Z) = \langle \delta[|\mathcal{A}_s| - |\mathcal{A}_s(Z)|] \rangle. \tag{28}$$

A straightforward calculation using the δ-function property

$$\delta(f(x)) = \sum_n \frac{1}{|f'(x_n)|} \delta(x - x_n), \tag{29}$$

where x_n is the nth root of $f(x)$, $f(x_n) = 0$, yields

$$\mathcal{P}(|\mathcal{A}_s|, Z) = \frac{\kappa\Gamma\, e^{1/\langle i_p \rangle}}{\langle i_p \rangle Z |\mathcal{A}_{s0}|} \left| \frac{\mathcal{A}_s}{\mathcal{A}_{s0}} \right|^{-1-\kappa\Gamma/\langle i_p \rangle Z} \times \theta(|\mathcal{A}_s| - |\mathcal{A}_{s0}| e^{Z/\kappa\Gamma}). \tag{30}$$

Here $\theta(x)$ is a unit step function. It can be easily verified that the PDF is normalized to unity at any $Z = \text{const}$ and Eq. (30) works for any $Z \neq 0$; it is singular at $Z = 0$ because $\mathcal{P}$ is a δ function at the source. We note in passing that a qualitatively similar form of PDF was derived for Stokes wave statistics in silica glass Raman amplifiers [17]. However, the long coherent memory of SRS in gases makes our system fundamentally different from silica glass Raman amplifiers with an instantaneous medium response. Further, we consider pump pulses with a strong coherent component superimposed with weak fluctuations, whereas the authors of [17] discuss the opposite regime of incoherent pump input.

The PDF of Eq. (30) is displayed in Fig. 1 in logarithmic scale at several propagation distances. It can be inferred from Eq. (30) that the PDF shape is determined by two factors. First, the unit step function describes a shift toward larger areas upon propagation due to the Stokes pulse amplification. Second, the power-law dependence is brought about by the noise transfer from the pump to the Stokes pulse in the course of SRS. Qualitatively, the interplay of these two trends fixes the Stokes area PDF shape. Further analysis of Eq. (30) reveals that the area PDF becomes so broad tailed that it ceases to attain finite

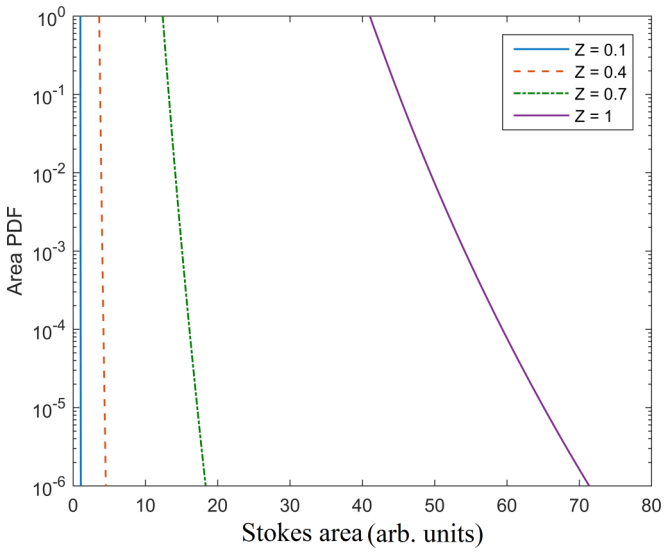

FIG. 1. Analytics: Stokes area PDF in the logarithmic scale at several propagation distances Z. The numerical values of the parameters are $T_p = 10^2 T_s$, $P_s = 10^{-3} P_p$, and $\Gamma = 0.24$.

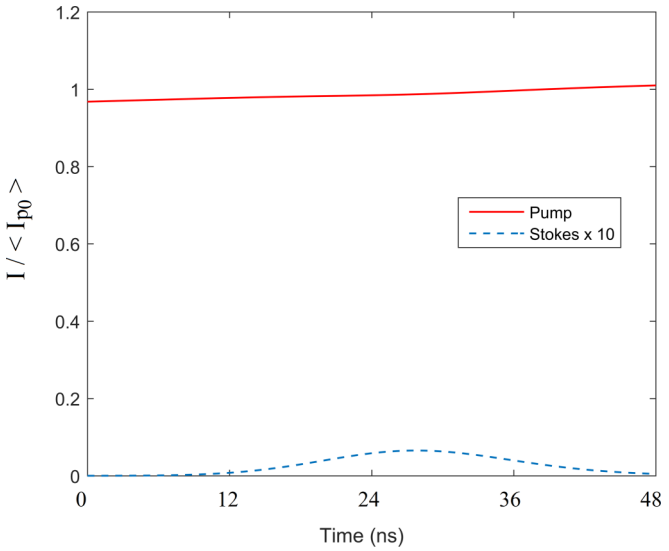

FIG. 2. Intensity profiles of the pump and Stokes modes at $Z = 0.3$. The numerical values of the parameters are $T_p = 10^2 T_s$, $P_s = 10^{-3} P_p$, and $\Gamma = 0.24$.

moments at the distances

$$Z \geqslant Z_* = \kappa\Gamma/\langle i_p \rangle, \tag{31}$$

estimating for our regime $\kappa \simeq 1$, $\Gamma \sim 1$, and $\langle i_p \rangle \sim 10^{-2}$, corresponding to 10% amplitude noise in the pump $z_* \sim 100 L_{\text{SRS}} \simeq 10$ cm. It follows from Eq. (31) that z_* is controlled by the pump noise intensity and coherent memory of the system; it can drop to a fraction of L_{SRS} for sufficiently long coherent memory times (small Γ) or noisy enough pump. Thus, rogue-wave-like phenomena can potentially unfold at very short propagation distances and be quantitatively described by our analytical theory. We stress that this conclusion is applicable to input Stokes pulses of any shape.

To test our UPA predictions, we carried out numerical simulations for the long intense pump case such that $T_p = 10^2 T_s$ and $P_s = 10^{-3} P_p$. We use $i_p = 10^{-2}$ and $\Gamma = 0.24$ in our numerical simulations. In Fig. 2 we display the average pump and Stokes pulse profiles at $Z = 0.3$ indicating that the UPA still holds at this propagation distance. We then exhibit the Stokes area PDF at several propagation distances and compare it with the corresponding analytical results in Fig. 3. It can be seen in the figure that while the theory and simulation agree very well up to $Z = 0.3$ for our pump noise level and coherent memory time, the two start deviating at $Z = 0.5$ and differ substantially at $Z = 0.7$. Thus the UPA breaks down rather quickly in this parameter regime. The ORW formation can occur at distances of the order $Z \sim 0.1$, though, provided coherent memory Γ^{-1} is boosted by two orders of magnitude for the same pump noise level. This can be achieved by increasing the pump intensity, for instance, which would incidentally extend the UPA applicability range. However, the true significance of our UPA theory lies in its ability to qualitatively predict the physical nature of the PDF transformation in SRS with noisy pump. We will use the gained insights to explain the emergence of non-Gaussian statistics beyond the UPA in the following section.

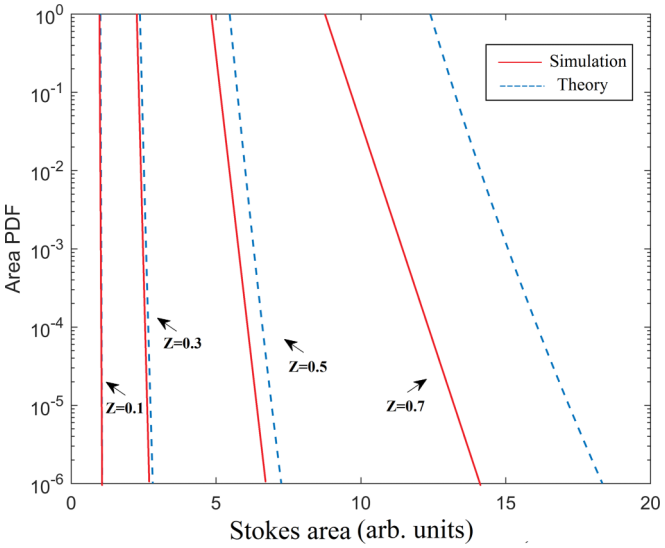

FIG. 3. Analytical versus numerical Stokes area PDF profiles at several propagation distances inside the fiber. The numerical values of the parameters are $T_p = 10^2 T_s$, $P_s = 10^{-3} P_p$, and $\Gamma = 0.24$.

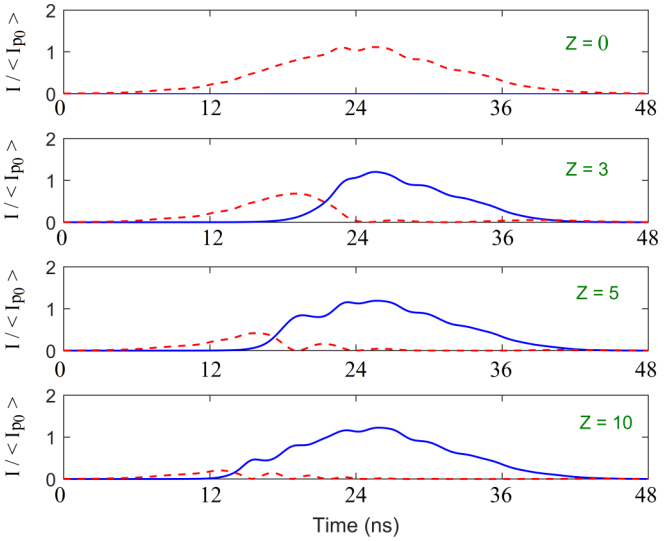

FIG. 4. Average intensity profiles of the pump (dashed line) and Stokes (solid line) pulses at several propagation distances. The coherent memory parameter is taken to be $\Gamma = 0.24$.

V. NON-GAUSSIAN STATISTICS BEYOND THE UNDEPLETED PUMP APPROXIMATION

We now numerically simulate SRS with fluctuating pump pulses beyond the UPA. As a generic realization of the system, we consider a hydrogen-filled HCPCF with typical parameters representative of the HCPCFs previously designed for SRS experiments [36]. The HCPCF has a low-loss transmission window between 1030 and 1150 nm. As a result, only the pump at $\lambda_p = 1064$ nm and first Stokes at $\lambda_s = 1134$ nm modes, interacting with the $J = 1$ to $J = 3$ rotational transition, can copropagate in the HCPCF. The coherent component of the pump is supplied by a $W_p = 100$ μJ laser operating at 1064 nm. The characteristic Raman interaction length and SRS interaction time are $L_{\rm SRS} = 1$ mm and $T_{\rm SRS} = 1.2$ ns, respectively. We assume the relaxation time of hydrogen in the HCPCF to be $\gamma^{-1} = 5$ ns [37]. The coherent memory parameter Γ is then $\Gamma = 0.24$; it can be controlled by adjusting the pump energy W_p. The input pump (coherent component) and Stokes pulses are assumed to be Gaussian of the same duration $t_p = t_s = t_* = 10$ ns, but the Stokes input is much weaker such that the Stokes input energy is just 1% of the pump one. The pump and Stokes pulses are centered at $t_0 = 24$ ns. We treat the pump source noise level, quantified by $\Delta P_p/P_p$, as a variable in our simulations.

In Fig. 4 we display the average intensities of the pump and Stokes pulses at several propagation distances. As is expected, the Stokes pulse intensity grows at the pump expense. Note characteristic oscillations experienced by both average intensity profiles, which are unambiguous signatures of a transient SRS regime. We then exhibit a time series of the peak Stokes power in Fig. 5(a) for $\Delta P_p/P_p = 0.3$ and in Fig. 5(b) for $\Delta P_p/P_p = 0.5$ at the fiber exit. It can be inferred from the figure that although extreme events do take place in both cases—the peak power reaches magnitudes around 20–40 times its average value at the fiber exit—the maximum attainable power level strongly depends on the pump noise level. In particular, the curve in Fig. 5(b) can be interpreted to represent a bona fide ORW with a peak pulse amplitude exceeding 6 times its average value at the fiber output.

Next we examine the Stokes power statistics in the present SRS regime. In Fig. 6 we exhibit the peak Stokes power PDF in logarithmic scale for the two cases: (a) relatively short system memory with $\Gamma = 0.97$ and (b) rather long system memory with $\Gamma = 0.24$. The peak Stokes power is evaluated at the fiber output and scaled to its average value there. The non-Gaussian behavior of the PDF is manifest in both cases on comparing it with a straight line Gaussian PDF of the peak pump power. Further, we can infer from Fig. 6 that the peak Stokes power PDF acquires a long tail and the tail extent markedly increases as the system coherent memory is enhanced. This is because the enhanced coherent memory implies that the SRS interaction is robust against medium dipole damping, thereby accommodating efficient noise transfer from the pump to the Stokes pulses. This point illustrates the crucial role the coherent memory effects play in ensuring that extreme events take place in the system. Finally, we exhibit the peak Stokes power PDF for rather coherent

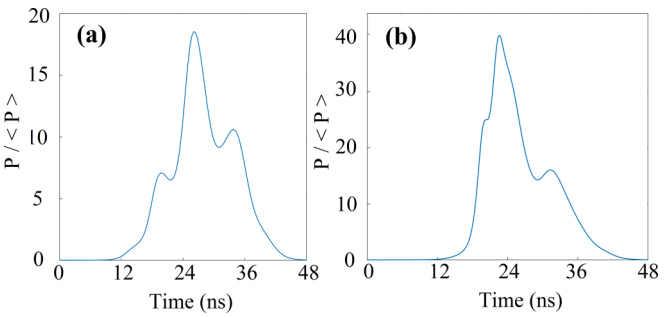

FIG. 5. Stokes pulse ensemble realization at the fiber exit for (a) $\Delta P_p/P_p = 0.3$ and (b) $\Delta P_p/P_p = 0.5$. The pulse power is scaled to the average power $\langle P \rangle$ at the fiber exit. In both cases, $\Gamma = 0.24$.

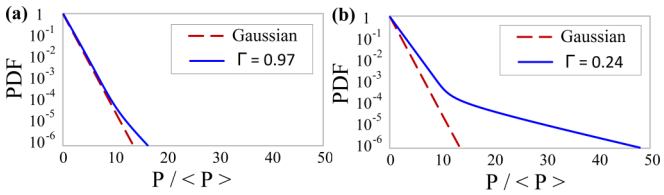

FIG. 6. Peak power PDF of a Stokes pulse ensemble at the fiber output for (a) relatively short, $\Gamma = 0.97$, and (b) rather long, $\Gamma = 0.24$, coherent memory times. The pulse power is scaled to the average power $\langle P \rangle$ at the fiber exit. The source noise level is $\Delta P_p / P_p = 0.5$.

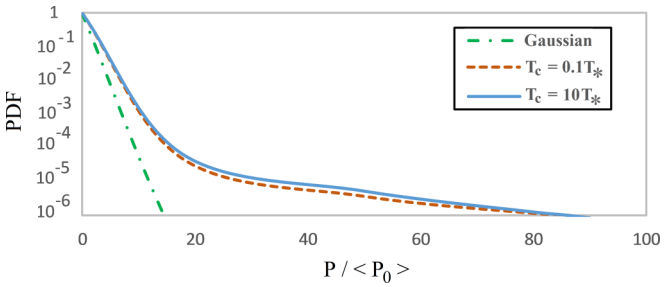

FIG. 7. Peak power PDF of a Stokes pulse ensemble at the fiber output for relatively coherent (solid line) and nearly incoherent (dashed line) sources. The pulse power is scaled to the average pump power $\langle P_0 \rangle$ at the source. The source noise level is $\Delta P_p / P_p = 0.01$ and $\Gamma = 0.24$.

and nearly incoherent pump sources in Fig. 7. It is evident from the figure that in sharp contrast to the noisy Stokes SRS case, the PDF in the present regime is virtually independent of the source pump coherence time. This circumstance can be explained by noting again the different physical origin of PDF tails, and hence ORW emergence, in the two SRS regimes that we have already discussed. Specifically, the PDF structure in the present situation depends solely on the amount of pump noise, but not on the noise particulars, including its spectrum and, by extension, its coherence time.

VI. SUMMARY

We explored the emergence of non-Gaussian statistics and optical rogue waves in stimulated Raman scattering in gases, focusing on a gas-filled, hollow-core photonic crystal fiber as a particular system realization. We specifically examined the role of coherent memory and source noise modeling in extreme event excitation in the system. We have demonstrated the crucial role that coherent memory plays in triggering heavy-tailed statistics of the system in the situations when the input Stokes or pump pulses are noisy. However, the non-Gaussian statistics emergence has fundamentally different physical origins in the two cases. On the one hand, we demonstrated earlier [22] that heavy-tailed statistics and ORWs result from the competition for the pump energy among coherent modes constituting a statistical Stokes input. On the other hand, we have shown here that the non-Gaussian statistics and ORW excitation in SRS with noisy pump can be attributed to noise transfer from the pump to initially coherent Stokes pulses. We have developed the analytical theory of such noise transfer in the system in the initial stage of SRS, well described within the undepleted pump approximation. We also discussed the parameter regime in which the emergent extreme events can be quantitatively described under the UPA. The insights gained enabled us to interpret our numerical findings beyond the undepleted pump approximation, which qualitatively follows the same scenario as was discovered under the UPA.

ACKNOWLEDGMENTS

The authors would like to thank Natural Sciences and Engineering Research Council of Canada (NSERC) and Killam Trusts for their support.

[1] A. I. Dyachenko and V. E. Zaklharov, Modulation instability of Stokes waves → freak wave, JETP Lett. **81**, 255 (2005).
[2] V. E. Zakharov, A. I. Dyachenko, and A. O. Prokofiev, Freak waves as nonlinear stage of Stokes wave modulation instability, Eur. J. Mech. B **25**, 677 (2006).
[3] C. Kharif, E. Pelinovsky, and A. Slunyaev, *Rogue Waves in the Ocean* (Springer, Berlin, 2009).
[4] M. Onorato, S. Residori, U. Bertolozzo, A. Montina, and F. T. Arecchi, Rogue waves and their generating mechanisms in different physical contexts, Phys. Rep. **528**, 47 (2013).
[5] J. M. Dudley, F. Dias, M. Erkintalo, and G. Genty, Instabilities, breathers, and rogue waves in optics, Nat. Photon. **9**, 306 (2015).
[6] N. Akhmediev *et al.*, Roadmap on optical rogue waves and extreme events, J. Opt. **18**, 063001 (2016).
[7] D. R. Solli, C. Ropers, P. Koonath, and B. Jalali, Optical rogue waves, Nature (London) **450**, 1054 (2007).
[8] M. Erkintalo, G. Genty, and J. M. Dudley, Rogue-wave-like characteristics in femtosecond supercontinuum generation, Opt. Lett. **34**, 2468 (2009).
[9] B. Kibler, C. Finot, and J. M. Dudley, Soliton and rogue wave statistics in supercontinuum generation with two zero dispersion wavelengths, Eur. Phys. J. **173**, 289 (2009).
[10] A. Montina, U. Bertolozzo, S. Residori, and F. T. Arecchi, Non-Gaussian Statistics and Extreme Waves in a Nonlinear Optical Cavity, Phys. Rev. Lett. **103**, 173901 (2009).
[11] S. Residori, U. Bertolozzo, A. Montina, F. Lenzini, and F. T. Arecchi, Rogue waves in spatially extended optical systems, Fluctuat. Noise Lett. **11**, 1240014 (2009).
[12] J. M. Soto-Crespo, P. Grelu, and N. Akhmediev, Dissipative rogue waves: Extreme pulses generated by passively mode-locked lasers, Phys. Rev. E **84**, 016604 (2011).
[13] A. Zavyalov, O. Egorov, R. Iliew, and F. Lederer, Rogue waves in mode-locked fiber lasers, Phys. Rev. A **85**, 013828 (2012).

[14] A. F. J. Runge, N. G. R. Broderick, and M. Erkintalo, Observation of soliton explosions in a passively mode-locked fiber laser, Optica **2**, 36 (2015).
[15] J. He, S. Xu, and K. Porsezian, New types of rogue wave in an erbium-doped fiber system, J. Phys. Soc. Jpn. **81**, 033002 (2012).
[16] K. Hammani, C. Finot, J. M. Dudley, and G. Millot, Optical rogue-wave-like extreme value fluctuations in fiber Raman amplifiers, Opt. Express **16**, 16467 (2008).
[17] K. Hammani, A. Picozzi, and C. Finot, Extreme statistics in Raman fiber amplifiers: From analytical description to experiments, Opt. Commun. **284**, 2594 (2011).
[18] J. Kasparian, P. Béjot, J.-P. Wolf, and J. M. Dudley, Optical rogue wave statistics in laser filamentation, Opt. Express **17**, 12070 (2009).
[19] D. Majus, V. Jukhna, G. Valiulis, D. Faccio, and A. Dubietis, Spatiotemporal rogue events in femtosecond filamentation, Phys. Rev. A **83**, 025802 (2011).
[20] P. M. Lushnikov and N. Vladimirova, Non-Gaussian statistics of multiple filamentation, Opt. Lett. **35**, 1965 (2010).
[21] K. Hammani, C. Finot, and G. Millot, Emergence of extreme events in fiber-based parametric processes driven by a partially incoherent pump wave, Opt. Lett. **34**, 1138 (2009).
[22] Y. E. Monfared and S. A. Ponomarenko, Non-Gaussian statistics and optical rogue waves in stimulated Raman scattering, Opt. Express **25**, 5941 (2017).
[23] F. T. Arecchi, U. Bertolozzo, A. Montina, and S. Residori, Granularity and Inhomogeneity are Joint Generators of Optical Rogue Waves, Phys. Rev. Lett. **106**, 153901 (2011).
[24] A. Picozzi, J. Garnier, T. Hanson, P. Suret, S. Randoux, G. Millot, and D. N. Christodoulides, Optical wave turbulence: Toward a unified thermodynamic formulation of statistical nonlinear optics, Phys. Rep. **542**, 1 (2014).
[25] K. Hammani, B. Kibler, C. Finot, and A. Picozzi, Emergence of rogue waves from optical turbulence, Phys. Lett. A **374**, 3585 (2010).
[26] B. Kibler, K. Hammani, C. Michel, C. Finot, and A. Picozzi, Rogue waves, rational solitons and wave turbulence theory, Phys. Lett. A **375**, 3149 (2011).
[27] S. Toenger, T. Godin, C. Billet, F. Dias, M. Erkintalo, G. Genty, and J. M. Dudley, Emergent rogue wave structures and statistics in spontaneous modulation instability, Sci. Rep. **5**, 10380 (2015).
[28] D. Agafontsev and V. E. Zakharov, Integrable turbulence and formation of rogue waves, Nonlinearity **28**, 2791 (2015).
[29] P. Walczak, S. Randoux, and P. Suret, Optical Rogue Waves in Integrable Turbulence, Phys. Rev. Lett. **114**, 143903 (2015).
[30] P. Suret, R. El Koussaifi, A. Tikan, C. Evain, S. Randoux, C. Szwaj, and S. Bielawski, Single-shot observation of optical rogue waves in integrable turbulence using microscopy, Nat. Commun. **7**, 13136 (2016).
[31] N. Akhmediev, J. M. Soto-Crespo, and N. Devine, Rogue waves, probability density functions and spectral features, Phys. Rev. E **94**, 022212 (2016)
[32] V. E. Zakharov, Turbulence in integrable systems, Stud. Appl. Math. **122**, 219 (2009).
[33] F. Y. F. Chu and A. C. Scott, Inverse scattering transform for wave-wave scattering, Phys. Rev. A **12**, 2060 (1975).
[34] D. J. Kaup, Physica D **19**, 125 (1986).
[35] J. W. Goodman, *Statistical Optics* (Wiley, New York, 1985).
[36] F. Benabid, G. Bouwmans, J. C. Knight, and P. St. J. Russell, Ultrahigh Efficiency Laser Wavelength Conversion in a Gas-Filled Hollow Core Photonic Crystal Fiber by Pure Stimulated Rotational Raman Scattering in Molecular Hydrogen, Phys. Rev. Lett. **93**, 123903 (2004).
[37] F. Flora and L. Giudicotti, Complete calibration of a Thomson scattering spectrometer system by rotational Raman scattering in H_2, Appl. Opt. **26**, 4001 (1987).
[38] F. Benabid and P. J. Roberts, Linear and nonlinear properties of photonic crystal fibers, J. Mod. Opt. **58**, 87 (2011).
[39] M. G. Raymer and J. Mostowski, Stimulated Raman scattering: Unified theory of spontaneous initiation and spatial propagation, Phys. Rev. A **24**, 1980 (1981).
[40] A. Nazarkin, A. Abdolvand, A. V. Chugreev, and P. St. J. Russell, Direct Observation of Self-Similarity in Evolution of Transient Stimulated Raman Scattering in Gas-Filled Photonic Crystal Fibers, Phys. Rev. Lett. **105**, 173902 (2010).
[41] R. W. Boyd, *Nonlinear Optics*, 2nd ed. (Academic, New York, 2003).
[42] M. Qasymeh, M. Cada, and S. A. Ponomarenko, Quadratic electro-optical Kerr effect: Application to photonic devices, IEEE J. Quantum Electron. **44**, 740 (2008).
[43] A. Ablovind, A. Nazarkin, A. V. Chugreev, C. F. Kaminski, and P. St. J. Russell, Solitary Pulse Generation by Backward Raman Scattering in H_2-Filled Photonic Crystal Fibers, Phys. Rev. Lett. **103**, 183902 (2009).
[44] L. Mandel and E. Wolf, *Optical Coherence and Quantum Optics* (Cambridge University Press, Cambridge, 1995).
[45] M. H. Frosz, Validation of input-noise model for simulations of supercontinuum generation and rogue waves, Opt. Express **18**, 14778 (2010).
[46] A. Papoulis, *Probability Random Variables, and Stochastic Processes*, 3rd ed. (McGraw-Hill, New York, 1991).
[47] L. Mokhtarpour and S. A. Ponomarenko, Fluctuating pulse propagation in resonant nonlinear media: Self-induced transparency random phase soliton formation, Opt. Express **23**, 30270 (2015).